

Differentially Flat Design of Under-Actuated Planar Robots: Experimental Results

Vivek Sangwan, Helge Kuebler and Sunil K. Agrawal

Abstract—Control of nonlinear under-actuated systems is an area of ongoing research. In certain applications, under-actuated systems are unavoidable. For instance, a biped can not have an actuator between the foot and the ground. In industrial robots, under-actuation can minimize cost and dead weight. Differential flatness, if applicable, provides a systematic approach to plan and control feasible trajectories for such systems. Recently, the authors have formulated a philosophy to design under-actuated planar manipulators that are differentially flat [1]. The design philosophy has two sufficient conditions: (i) an inertia distribution scheme, and (ii) an actuator and torque spring placement scheme. The philosophy covers a broad range of n -DOF manipulator designs with the degree of under-actuation varying from 1 to $n-1$ as opposed to under-actuation by one or two in most of the literature on under-actuated manipulators. This paper presents a 3-DOF planar manipulator designed on the basis of this philosophy and an experimental study of controllers based on its differential flatness property. It is demonstrated experimentally that the differential flatness based controllers are able to track the desired trajectories with small tracking errors even in the presence of disturbances like friction, parameter uncertainty etc. It is shown via simulation that the errors observed in the trajectories can be attributed to the friction present at the unactuated joint.

I. INTRODUCTION

Under-actuated systems arise in numerous situations. In certain applications, such as, walking robots it is unavoidable as there can not be an actuator between the foot and the ground [2]–[5]. Under-actuation can be a better design choice for robots in space and industrial applications [6], [7] due to cost and dead-weight considerations. Other interesting robotic applications of under-actuation include the Acrobot [8], [9], the gymnast robots [10], the brachiating robots [11], and surgical robots [12]. Another instance where under-actuation finds application is in restoring operation in spite of actuator failure [13], [14].

The mathematical complexity and wide variety of applications have kept under-actuated systems an area of active research. Arai et al. [15] have shown a 3-DOF planar manipulator with passive last joint to be controllable by a constructive method. They have constructed the trajectories between arbitrary terminal states by considering the motion of center of percussion of the link. A proof of controllability

V. Sangwan is a PhD student with Department of Mechanical Engineering, University of Delaware, Newark, DE 19716, USA sangwan@udel.edu

H. Kuebler is a visiting Researcher from University of Stuttgart, Germany to Department of Mechanical Engineering, University of Delaware Newark, DE 19716, USA. kuebler@udel.edu

S. K. Agrawal is a Professor of Mechanical Engineering with Department of Mechanical Engineering, University of Delaware, Newark, DE 19716, USA agrawal@udel.edu

for n -link manipulator having only one passive joint, not at the inertially fixed joint, has been presented by Kobayashi et al. [16]. Luca et al. [17] have reported another study with single under-actuation at the last joint for planar manipulators, based on the center of percussion of the last joint. Controllability properties of 3-DOF RRR and PPR manipulators for all possible locations of the single passive joint has been studied by Mahindrakar et al. [18]. Control paradigms for n -link planar manipulators with a passive first joint has been reported by Grizzle et al. [19].

For a fully actuated robot, as long as the joint inputs are allowed to be unlimited, there are no theoretical restrictions in joint trajectories that can be achieved by the system. However, if the system is under-actuated, not all joint trajectories are attainable by the system, i.e., only such joint trajectories are valid that do not require inputs at the joints where the actuators are missing. This implies that the system might not be able to traverse between two arbitrary states hence might not be controllable. In theory, it may be possible to characterize the joint trajectories attainable by the under-actuated system by forward numerical integration, where the actuator inputs at the joints have been specified. However, it is not possible to analytically characterize the input-output relation since the governing differential equations are coupled and nonlinear. Differential flatness, if applicable, provides a systematic approach to plan and control feasible trajectories for such systems.

Agrawal et al. [6], [7] have presented inertia redistribution techniques to design under-actuated space robots. Recently, they extended the inertia redistribution technique to a general planar n -DOF under-actuated planar manipulators and formulated a philosophy to design under-actuated planar manipulators that are differentially flat [1]. The design philosophy has two sufficient conditions: (i) an inertia distribution scheme, and (ii) an actuator and torque spring placement scheme. For a planar manipulator with n -links connected to a fixed base by n revolute joints, the inertia distribution scheme is the following recursive center-of-mass placement: (i) the center of mass of the last link n is on joint axis n , (ii) the center of mass of the last two links n and $n-1$ lies on the joint axis $n-1$, (iii) this procedure repeats until the center of mass of the last j links, i.e., $n, n-1, \dots, n-j+1$ is on the joint axis $n-j+1$. The actuator and torque spring placement scheme for this system with special mass distribution in its last j bodies is as follows: The first $n-j+1$ joints have actuators while the remaining $j-1$ joints are passive but have torsional springs. This system is under-actuated by $j-1$, where $j \geq 2$. It is quite important to

note that j can take values from 2 to n . This covers a broad range of designs with the degree of under-actuation varying from 1 to $n - 1$ as opposed to underactuation by one or two in most of the literature on under-actuated manipulators. Also, this design philosophy is not restricted only to under-actuated manipulators but has also been applied successfully to bipedal walking robots [20].

This paper presents an experimental study of controllers, based on differential flatness property of the planar manipulators designed based on the philosophy presented by the authors previously [1]. The authors realized while conducting the experiments reported in this paper, that, the center-of-mass placement conditions can be met very accurately by having a movable counter mass. The key contributions of this paper are as follows: (i) A 3-DOF planar under-actuated robot that is fabricated following the design philosophy presented earlier in [1]. (ii) It is demonstrated experimentally that the differential flatness based controllers are able to track the desired trajectories with small tracking errors even in the presence disturbances like friction, parameter uncertainty etc. (iii) It is shown via simulation that the errors observed in the trajectories can be attributed to the friction present at the unactuated joint.

The organization of this paper is as follows: Section II presents the details of the manipulator and the experimental setup. The differentially flat dynamic model of the manipulator along with the flat outputs and corresponding state and input transformations are presented in section III. The experimental and simulation results are presented in section IV followed by conclusions and future work in section V

II. THE DIFFERENTIALLY FLAT 3-DOF MANIPULATOR

In this paper, we are studying the effectiveness of the flatness based controller with a three degree-of-freedom, planar open-chain robot shown in Figs. 1 and 2. Here, $n = 3$ and $j = 2$, i.e. the center of mass of link 3 is on joint 3 and center of mass of links 2 and 3 is on joint 2. This center-of-mass placement is done experimentally by means of movable counter masses on links 2 and 3. The counters masses shown in Fig. 2 can be moved up or down until the link is in equilibrium in every orientation. It is under-actuated, with actuators only at the first and second joint. The actuators used are brushed DC motors with gearboxes. The third joint is passive, with a torque spring attached to it. Each of the joint has an optical digital incremental encoder to measure the angle and there are torque sensors between the motor output shaft and the robot joint to measure the torque being supplied to the motor. Software and hardware from National Instruments is used to implement the controllers. We assume that the robot's goal is to pass through a given set of states at specified time instants. Such a situation can be encountered in assembling components in industry. Similar planning and control paradigms can be used for set point control and cyclic trajectories.

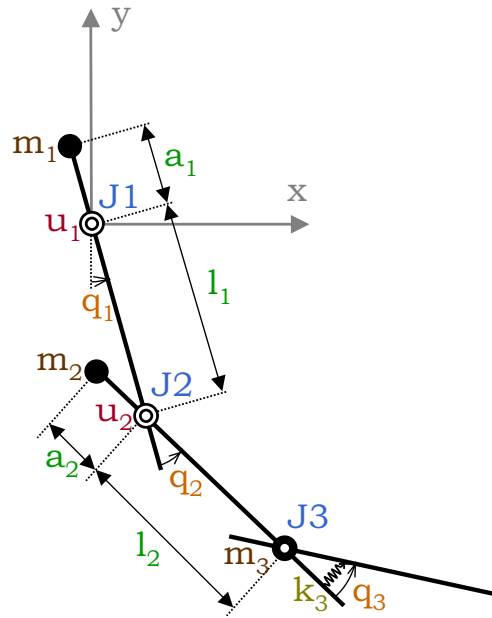


Fig. 1. A 3-DOF planar robot. The first two joints are actuated and the last joint is passive with a torque spring. A small circle on each link denotes the COM. The COM of the third link is at joint three and the COM of links two and three is at joint two. This is done using a counter mass on link two.

TABLE I
THE SYSTEM PARAMETERS

Link(i)	m_i (kg)	l_i (m)	a_i (m)	I_i (kgm ²)
1	5.548	0.283	0.0762	0.1025
2	1.905	0.219	0.0520	0.0383
3	0.452	0.150	0	0.0015

A. System Parameter Estimation

In order to implement a flatness based controller, the parameters of the arm (see Fig. 1) have to be well known. While this is fairly simple for m_i and l_i , the moments of inertia of the three links are estimated experimentally by using simple pendulum experiments. First, the time constants of the oscillations are measured. Then, the moments of inertia can be determined by using the time period equation and the parallel axis theorem. The Center-Of-Mass (COM) locations a_1 and a_2 are automatically determined while balancing link 1 and link 2. The stiffness constant k_3 was determined to be 0.07Nm/rad by applying known loads and measuring the deflection of the torque spring and then finding the slope of the torque load vs. displacement graph. Table I presents the inertia and length parameters of the system.

III. DIFFERENTIALLY FLAT DYNAMICS

The equations of motion for the system in the ideal frictionless situation are given by:

$$A\ddot{q} + g(q_1) = u, \quad (1)$$

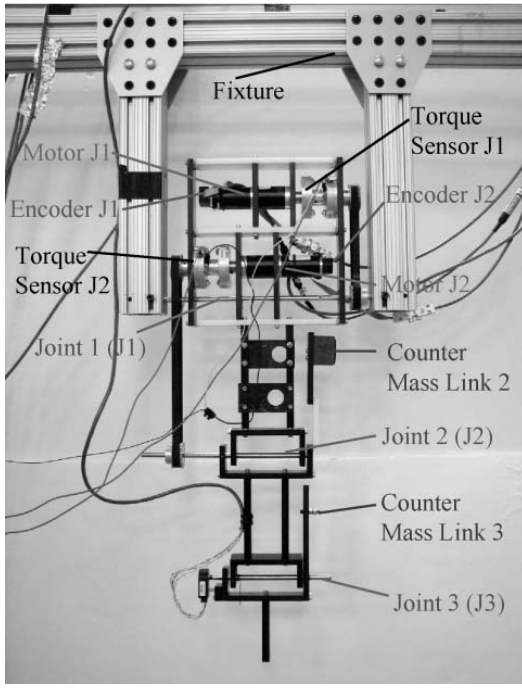


Fig. 2. The 3-DOF robotic arm. There are movable counter masses on the last two links to accurately position the COM. All three joints have incremental encoders to measure the angular position. First two joints have DC motors with torque sensors mounted at the output shaft of the gearboxes. Steel shafts along with roller bearings are used to make low friction and rigid revolute joints. The robot is made out of delrin and weighs around 8 Kgs. National Instruments' software LabVIEW and a real-time PXI target is used to implement the controller.

where A is the symmetric and positive definite inertia matrix and $g(q_1)$ is the potential term for this special inertia distribution for the last two joints, and u is the input vector given by:

$$A = \begin{bmatrix} a_{11} & a_{22} & a_{33} \\ a_{22} & a_{22} & a_{33} \\ a_{33} & a_{33} & a_{33} \end{bmatrix}, \quad (2)$$

where $a_{11} = I_1 + I_2 + I_3 + m_1 a_1^2 + m_2 (l_1^2 + a_2^2) + m_3 (l_1^2 + l_2^2)$, $a_{22} = I_2 + I_3 + m_2 a_2^2 + m_3 l_2^2$, and $a_{33} = I_3$.

$$g(q_1) = \begin{bmatrix} (m_1 a_1 + m_2 l_1 + m_3 l_1) g \sin(q_1) \\ 0 \\ k_3 q_3 \end{bmatrix}, \quad (3)$$

$$u = \begin{bmatrix} u_1 \\ u_2 \\ 0 \end{bmatrix}, q = \begin{bmatrix} q_1 \\ q_2 \\ q_3 \end{bmatrix}. \quad (4)$$

In general, the inertial matrix does not depend on q_1 . In this case, due to the special mass distribution, it does not depend on q_2 and q_3 as well and hence is a constant. Since, the inertia matrix is constant there are no coriolis terms in the equation. Also, we can observe the special structure of the inertia matrix discussed in the previous section. It was realized while conducting the experiments that the center-of-mass placement conditions can be met very accurately by having a movable counter-mass. It has been shown earlier [1]

that the system is flat and the flat outputs can be selected as $y = [q_1, (q_1 + q_2 + q_3)]$ having relative degree $[2, 4]$ with a sum of 6, the number of states. The diffeomorphism between the states, inputs and flat output function and their derivatives for the frictionless case is given by:

$$\begin{bmatrix} q_1 \\ q_2 \\ q_3 \\ \dot{q}_1 \\ \dot{q}_2 \\ \dot{q}_3 \end{bmatrix} = \begin{bmatrix} 1 & 0 & 0 & 0 & 0 & 0 \\ -1 & 1 & 0 & 0 & \frac{a_{33}}{k_3} & 0 \\ 0 & 0 & 0 & 0 & -\frac{a_{33}}{k_3} & 0 \\ 0 & 0 & 1 & 0 & 0 & 0 \\ 0 & 0 & -1 & 1 & 0 & \frac{a_{33}}{k_3} \\ 0 & 0 & 0 & 0 & 0 & -\frac{a_{33}}{k_3} \end{bmatrix} \begin{bmatrix} y_1 \\ y_2 \\ \dot{y}_1 \\ \dot{y}_2 \\ \ddot{y}_2 \\ y_2^{(3)} \end{bmatrix},$$

$$u_1 = u_2 + (a_{11} - a_{22})\ddot{y}_1 + (m_1 a_1 + m_2 l_1 + m_3 l_1)g \cos(y_1),$$

$$u_2 = \frac{a_{33}(a_{22} - a_{33})y_2^{(4)}}{k_3} + a_{22}\ddot{y}_2. \quad (5)$$

A. Planning And Control

A useful task for a robot is to traverse through a given sequence of state points at specified time instants. For the ideal differentially flat system, any output trajectory is consistent with the dynamics. Also, for such a system, there exists a diffeomorphism between the system state and flat outputs and their derivatives. Following steps were taken to plan the trajectories: (i) We selected a set of states containing four different six-dimensional state vectors. The first and last states are chosen to zero angular velocities. (ii) Using the diffeomorphism, the selected sequence of system states is transformed into the flat outputs and their derivatives. (iii) Using polynomials, a trajectory is constructed satisfying the output and output derivative constraints at all the time instants. (iv) The trajectories parameterized in terms of polynomials were optimized using Sequential Quadratic Programming (SQP) based optimization routines to minimize the energy consumption and to satisfy constraints on torques and maximum angular excursions. More details about the planning algorithm were presented earlier [1], [20]. First, we define a new set of inputs given by $v_1 = \ddot{y}_1$ and $v_2 = y_2^{(4)}$. Each of the new control inputs are computed using (7).

$$v_1 = \ddot{y}_{1d} + K_{11}(\dot{y}_{1d} - \dot{y}_1) + K_{12}(y_{1d} - y_1), \quad (6)$$

$$v_2 = y_{2d}^{(4)} + K_{21}(y_{2d}^{(3)} - y_2^{(3)}) + \dots + K_{24}(y_{2d} - y_2). \quad (7)$$

The subscript d in (7) denotes the planned trajectories. The actual inputs can be computed using the diffeomorphism (5). For all the experiments conducted in this paper the initial set of gains were chosen such that all the poles are placed at -5 and then they had to be handtuned slightly while conducting the experiments with each of the cases presented. The encoders had a resolution of 500 counts/rev (CPR) for the first two joints and a resolution of 1250 CPR for the third joint. The encoder signals were differentiated once and then filtered using first order filter to get the angular velocities. The actuators used are brushed DC motors with a reduction ratio of 156 from Maxon. A rapid control prototyper NI PXI-8196 was used to do the control implementation with a sampling time of $1ms$.

IV. RESULTS AND DISCUSSION

This section presents the experimental results from the tracking experiments with the 3-DOF robot. The desired trajectories for the outputs $y_{1,des}$ and $y_{2,des}$ were obtained using the planner described in the previous section. Using the diffeomorphism, the desired output trajectories can also be converted to corresponding desired state trajectories q_{des} and \dot{q}_{des} . Three different types of controllers were implemented on the 3-DOF robot. Following are the implementation details and results from each of those:

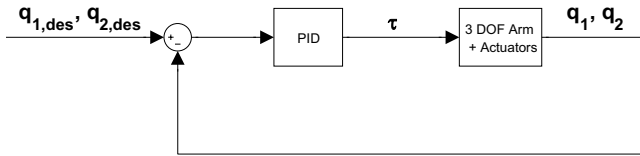


Fig. 3. Tracking of q_1 and q_2 by a simple PID position controller.

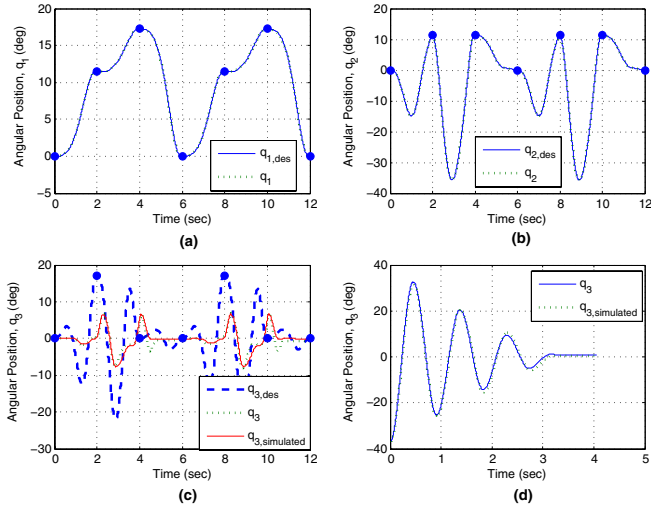


Fig. 4. Tracking results for the q_1 and q_2 position control. In these experiments no feedback is used from the third joint. It is clear that with this controller, q_1 and q_2 track very well but the performance of q_3 is unacceptable. Subfigure (d) presents a set of data used to determine a friction model for the unactuated joint.

1) *Position Control*: First, a simple PID control for the first two joints was implemented, as shown in Fig. 3. The desired trajectories for the first two joints were used as the reference signal. This controller is effectively an open loop controller for the unactuated joint since there is no feedback from the third joint. The results in Fig. 4 clearly demonstrate that the first two joint trajectories are tracked very well but tracking for the third joint is unacceptable. In theory, the third joint will also track the corresponding desired trajectory if: (i) the first two joints track exactly, and (ii) the dynamic model (1) is very accurate, this also implies that the robot does not have friction, and (iii) corresponding parameters are known exactly. With this controller the first condition is met reasonably but the other two conditions are hard to satisfy.

While doing the experiments the authors realized that the COM placement conditions could be satisfied accurately but there was a small friction at the unactuated joint. A friction model for the third unactuated joint containing static friction and viscous friction terms was determined experimentally through damped simple pendulum experiments. A representative set of data is presented in Fig. 4d. The system dynamics was simulated along with the experimentally determined friction model. The simulated trajectory is overlaid on the measured and desired trajectories in Fig. 4c. It can be clearly seen that the friction explains the observed response for the third unactuated joint. The flatness based controllers incorporate a feedback from the third joint as well and hence are expected to improve the performance.

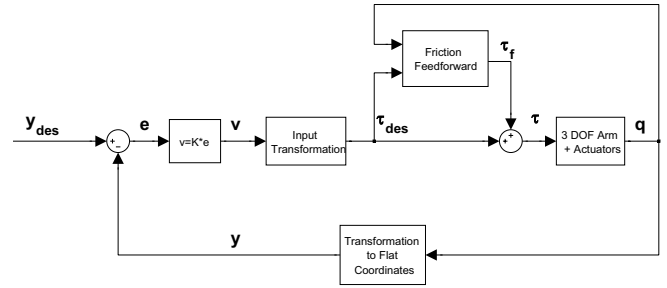
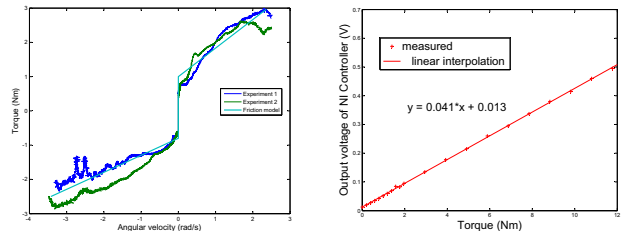


Fig. 5. A flatness based torque controller with friction feedforward to track the two outputs. Friction feedforward is used to overcome the effects of friction at the actuated joints predominantly due to the gearboxes in the motors.



(a) The experimental data of friction torque in the motor and gearbox as a function of the angular velocity and the nonlinear friction model.

(b) Experimental data to determine the relationship between the voltage input to the amplifier and the torque output of the motor.

Fig. 6. Experiments to determine the model of the DC motors with gearboxes.

2) *Flatness Based Torque Controller Using Motor Torque Constant And Friction Feedforward*: A flatness based controller generates torque commands for the robot. Due to the presence of friction in the gearbox, the relationship between the voltage input and torque output for the motor is nonlinear. The friction model was experimentally determined using the method described in [21]. A representative set of data as well the friction model are shown in Fig. 6a. This model is used to cancel the friction present in the gearbox by feedforward.

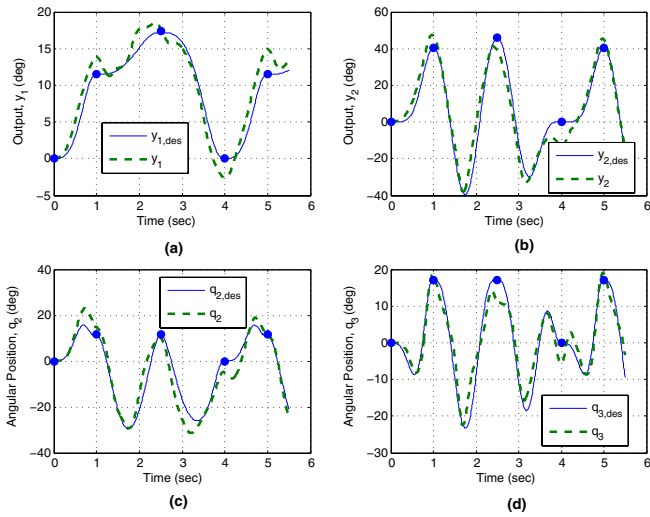


Fig. 7. Tracking results for the flatness based controller with friction feedforward. It is evident that there are small tracking errors for the output and angular position trajectories and the tracking has significantly improved for the third joint.

Also, to be able to apply a voltage representing a required torque level, it is important to know the relationship between input voltage and the torque output for the DC motors. This is also determined experimentally by applying a known voltage to the amplifier and stalling the motor by adding known weights at the end of a cantilever attached to the output shaft. A stall torque vs applied voltage plot for the motor is presented in Fig. 6b. The slope of the linear relationship was determined and used in the controller. The tracking results are presented in Fig. 7. It is evident that there are small tracking errors for the output and angular position trajectories and the tracking has significantly improved for the third joint.

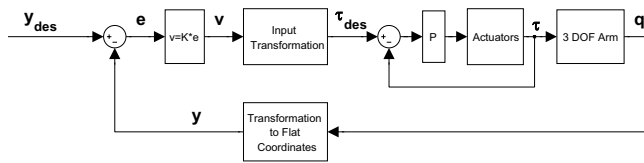


Fig. 8. A flatness based torque controller with an inner torque feedback control loop. The inner torque feedback loop provides a tighter control over the torque seen by the joints.

3) Flatness Based Controller With Torque Inner Loop:

In general, friction is very hard to model and there can be inaccuracies in the experimental determination of the model. Hence, a performance improvement can be expected if the technique of providing a required torque input to the robot is improved. The strategy adopted by the authors is to close a loop on the torque at the gearbox output shaft using a torque sensor. The placement of the torque sensor is shown in Fig. 2. A proportional controller is used for the inner torque feedback loop as shown in Fig. 8. The inner torque loop eliminates all the nonlinear effects due to the gearbox and provides a tighter control on the friction seen by the

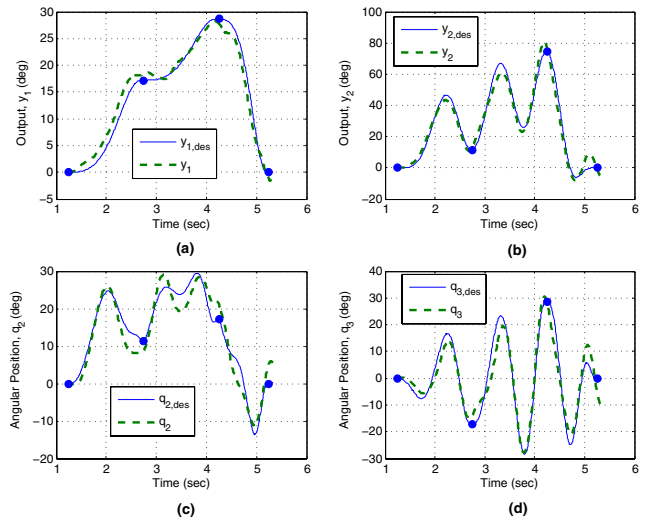


Fig. 9. Tracking results for the flatness based controller with inner torque feedback control loop. The tracking performance looks slightly better than the controller with friction feedforward.

robot. It should be noted that there is still some damping left at the revolute joints due to the bearings, hanging wires etc. Tracking results for the flatness based controller with inner torque feedback control loop are shown in Fig. 9. The tracking performance looks slightly better than the controller with friction feedforward.

Results from the two flatness based controllers suggest that, for under-actuated robots flatness based controllers give small tracking errors in the individual output trajectories but because of feedback from all the joints, control over unactuated joints is significantly enhanced.

V. CONCLUSIONS AND FUTURE WORKS

The authors have previously established [1] that a class of under-actuated planar open chain robots with a specific inertia distribution along with a specific arrangement of springs and actuators exhibit the property of differential flatness under frictionless conditions. Once this property is established, any output trajectory is consistent with the dynamics of the under-actuated system. This also ensures that one can plan a point-to-point maneuver between any two arbitrary points in its state space.

In this paper, a 3-DOF planar under-actuated robot is presented that is fabricated following the differentially flat design philosophy. The effectiveness of controllers based on differential flatness of the under-actuated manipulators in the presence of friction and other uncertainties is studied experimentally. Experiments with a 3-DOF manipulator are performed with three different types of controllers: (i) a simple position control with feedback from the first two joints only, (ii) a flatness based torque controller using the motor torque constant and friction feedforward with feedback from all three joints, (iii) a flatness based torque controller with an outer loop with feedback from all three joints and

an inner torque loop with feedback from the torque sensors at the two actuated joints.

Results from the first controller when compared with the other two controllers show that flatness based controllers perform much better than simple position control of actuated joints. Results from the two flatness based controllers suggest that for under-actuated robots, flatness based controllers give small tracking errors in the individual output trajectories but because of feedback from all the joints, control over unactuated joints is significantly enhanced. The coefficient of friction was estimated experimentally and the deviation of the system response from the response of a frictionless differentially flat system could be satisfactorily explained by simulating the position controller for the robot with experimentally determined friction model.

It is also noted that the performance of the unactuated system can be improved by (i) reducing the friction in the joints with a better design and/or, (ii) making the contribution of friction torque small compared to other contributions e.g. performing high speed motion which increases the contribution of inertial torques or by adding more mass and stiffness.

In future, the authors wish to make design improvements in the 3-DOF robot, e.g. added mass and stiffness to reduce the contribution of friction. Experiments to quantify performance in the entire workspace and to study the effects of payload will be performed. Applicability of variable structure robust control and adaptive control strategy will be investigated. Also, extension of these ideas to three dimensional manipulators can also be very fruitful, as already shown in differentially flat space robots [6], [7].

VI. ACKNOWLEDGMENTS

The authors gratefully acknowledge Prof. Oliver Sawodny and Prof. Michael Zeitz at University of Stuttgart for the email conversations about flatness and Konrad Adenauer Foundation, Germany for funding Helge's visit to Mechanical Systems Laboratory, University of Delaware. The authors would also like to thank PhD students Sai Banala and Jichul Ryu at Department of Mechanical Engineering, University of Delaware for their valuable suggestions and undergraduate student Khenya Still at Department of Mechanical Engineering, University of Delaware for helping with robot fabrication.

REFERENCES

- [1] S. K. Agrawal and V. Sangwan, "Design of under-actuated open-chain planar robots for repetitive cyclic motions," in *Proceedings of the ASME Design Engineering Technical Conference*, Philadelphia, PA, USA, Sept 2006.
- [2] M. H. Raibert, *Legged Robots That Balance*, 1st ed. Massachusetts, USA: The MIT Press, 1986.
- [3] M. Vukobratovic, B. Borovac, D. Surla, and D. Stokic, *Biped Locomotion: Dynamics, Stability, Control & Application*, 1st ed. Berlin, Germany: Springer-Verlag, 1990.
- [4] T. McGeer, "Passive dynamic walking," *The International Journal of Robotics Research*, vol. 9, no. 2, pp. 62–82, 1990.
- [5] C. Chevallereau, "A time-scaling control for an under actuated biped robot," *IEEE Transactions on Robotics and Automation*, vol. 19, no. 2, pp. 362–368, 2003.

- [6] S. K. Agrawal, K. Pathak, J. Franch, R. Lampariello, and G. Hirzinger, "Design of a differentially flat open-chain space robot with arbitrarily oriented joints and two momentum wheels," in *Proceedings IEEE International Conference on Robotics and Automation (ICRA'06)*, Orlando, FL, USA, May 2006, pp. 3867–3872.
- [7] J. Franch, S. K. Agrawal, A. Fattah, and S. Oh, "Design of differentially flat planar space robots: A step forward in their planning and control," in *Proceedings IEEE International Conference on Intelligent Robots and Systems (IROS'03)*, Las Vegas, NV, United States, Oct 2003, pp. 3053–3058.
- [8] M. D. Berkemeier and R. S. Fearing, "Tracking fast inverted trajectories of the underactuated acrobot," *IEEE Transactions on Robotics and Automation*, vol. 15, no. 4, pp. 740–750, Aug. 1999.
- [9] M. W. Spong, "The swing up control problem for the acrobot," *IEEE Control Systems Magazine*, vol. 15, no. 1, pp. 49–55, Feb. 1995.
- [10] K. Ono, K. Yamamoto, and A. Imadu, "Control of giant swing motion of a two-link horizontal bar gymnastic robot," *Advanced Robotics*, vol. 15, no. 4, pp. 449–465, July 2001.
- [11] J. Nakanishi, T. Fukuda, and D. Koditschek, "A brachiating robot controller," *IEEE Transactions on Robotics and Automation*, vol. 16, no. 2, pp. 109–123, April 2000.
- [12] J. Funda, R. Taylor, B. Eldridge, S. Gomory, and K. Gruben, "Constrained cartesian motion control for teleoperated surgicalrobots," *IEEE Transactions on Robotics and Automation*, vol. 12, no. 3, pp. 453–465, June 1996.
- [13] H. Arai and S. Tachi, "Position control of a manipulator with passive joints using dynamic coupling," *IEEE Transactions on Robotics and Automation*, vol. 7, no. 4, pp. 528–534, Aug 1991.
- [14] J. Shin and J. Lee, "Trajectory planning and robust adaptive control for under-actuated manipulators," *Electronics Letters*, vol. 34, no. 17, pp. 1705–1706, Aug 1998.
- [15] H. Arai, K. Tanie, and N. Shiroma, "Nonholonomic control of a three-dof planar under-actuated manipulator," *IEEE Transactions on Robotics and Automation*, vol. 14, no. 5, pp. 681–695, Oct 1998.
- [16] K. Kobayashi and T. Yoshikawa, "Controllability of under-actuated planar manipulators with one unactuated joint," *The International Journal of Robotics Research*, vol. 21, no. 5-6, pp. 555–561, 2002.
- [17] A. D. Luca and G. Oriolo, "Trajectory planning and control for planar robots with passive last joint," *The International Journal of Robotics Research*, vol. 21, no. 5-6, pp. 575–590, 2002.
- [18] A. D. Mahindrakar, R. Banavar, and M. Reyhanoglu, "Controllability and point-to-point control of 3-dof planar horizontal underactuated manipulators," *International Journal of Control*, vol. 78, no. 1, pp. 1–13, Jan 2005.
- [19] J. Grizzle, C. H. Moog, and C. Chevallereau, "Nonlinear control of mechanical systems with an unactuated cyclic variable," *IEEE Transactions on Automatic Control*, vol. 50, no. 5, pp. 559–576, May 2005.
- [20] V. Sangwan and S. K. Agrawal, "Differentially flat design of bipeds ensuring limit-cycles," in *Proceedings IEEE International Conference on Robotics and Automation (ICRA'07)*, Rome, Italy, Apr 2007.
- [21] S. K. Agrawal, S. K. Banala, A. Fattah, V. Sangwan, V. Krishnamoorthy, J. P. Scholz, and W.-L. Hsu, "Assessment of motion of a swing leg and gait rehabilitation with a gravity balancing exoskeleton," *The IEEE Transactions on Neural systems and Rehabilitation Engineering*, 2007.